DOI: 10.1021/ic1018778

Inorganic Chemistry
Article

Synthesis, Composition, and Structure of Sillenite-Type Solid Solutions in the $Bi_2O_3-SiO_2-MnO_2$ System

Tatyana I. Mel'nikova,*,† Galina M. Kuz'micheva,† Victor B. Rybakov,‡ Nadezhda B. Bolotina,§ and Alexander B. Dubovsky⊥

†*Lomonosov State Academy of Fine Chemical Technology, Moscow, 119571 Russia,* ‡*Moscow State University, Moscow, 119991 Russia,* §*Shubnikov Institute of Crystallography, Russian Academy of Sciences, Moscow, 119333 Russia, and* ⊥*Moscow State Open University, Aleksandrov, 601650 Russia*

Received September 12, 2010

Individual compounds and solid solutions are obtained under hydrothermal conditions in the $Bi_2O_3-SiO_2-MnO_2$ system in the form of faceted crystals and epitaxial films on the $Bi_{24}Si_2O_{40}$ substrate. The crystals have the shape of a cube (for the molar ratio of the starting components $Na_2SiO_3 \cdot 9H_2O:Mn(NO_3)_2 \cdot 6H_2O > 1$), a tetrahedron (for $Na_2SiO_3 \cdot 9H_2O:Mn(NO_3)_2 \cdot 6H_2O < 1$), or a tetrahedron−cube combination (for $Na_2SiO_3 \cdot 9H_2O:Mn(NO_3)_2 \cdot 6H_2O = 1$). Crystal−chemical analysis based on the data of single-crystal and powder X-ray diffraction, IR spectra, and the results of calculation of the local balance by the bond-valence method reveals formation of the $Bi_{24}(Si^{4+},Mn^{4+})_2O_{40}$ phases, which probably include Mn^{5+} ions (epitaxial films), as well as the $Bi_{24}(Si^{4+},Bi^{3+},Mn^{4+})_2O_{40}$ and $Bi_{24}(Si^{4+},Mn^{4+})_2O_{40}$ phases in the $(1-x)Bi^{3+}{}_{24}Si^{4+}{}_2O_{40} - x(Bi^{3+}{}_{24}Mn^{4+}{}_2O_{40})$ system and the $Bi_{24}(Bi^{3+},Mn^{4+})_2O_{40}$ phase in the $(1-x)Bi^{3+}{}_{24}Bi^{3+}{}_2(O_{39}\square_1) - x(Bi^{3+}{}_{24}Mn^{4+}{}_2O_{40})$ system. Precision X-ray diffraction studies of single crystals of the $Bi_{24}(Bi,Si,Mn)_2O_{40}$ general composition show that these sillenites crystallize in space group *P*23 and not *I*23 as the $Bi_{24}Si_2O_{40}$ phase. The dissymmetrization of sillenite phases is observed for the first time. It is explained by a kinetic (growth) phase transition of the order−disorder type due to population of a crystallographic site by atoms with different crystal−chemical properties and quasi-equilibrium conditions of crystal growth in the course of a hydrothermal synthesis below 400 °C at unequal molar amounts of the starting components in the batch.

Introduction

Compounds $Bi_{24}M_2O_{40}$ belong to the sillenite family and crystallize in the γ-Bi_2O_3 structural type, $z = 13$ ($Bi_{12}BiO_{20-\delta}$, $z = 2$, or $Bi_{24}Bi_2O_{40-\delta}$, $z = 1$), space group *I*23.[1] The Bi1 atom occupies a 24f site ($x \sim 0.17$, $y \sim 0.32$, and $z \sim 0.01$). Its coordination number (CN) is 5, and the coordination polyhedron (CP) is a distorted semioctahedron BiO_5. The M atom occupies the Bi2 (2a) position at the origin; CN = 4, and CP is a tetrahedron MO_4. The O2 and O3 atoms are located at the 3-fold axes (8c sites), and the O1 atom occupies a 24f site (Figure 1a).

A specific structure allows one to obtain $Bi_{24}M_2O_{40}$ sillenites of different compositions (varying M atoms) and their solid solutions $Bi_{24}(M',M'')_2O_{40}$. The tetrahedral M position can be populated by not only ions with suitable crystal−chemical properties (e.g., Si^{4+}, Ge^{4+}, or Cr^{4+}) but ions that enter into this site as a result of self-organization (e.g., Ti^{4+} or V^{5+}) as well. As a result, about 60 individual compounds and a large number of various solid solutions on their base were obtained. They form the sillenite family.[2]

Compounds of the sillenite family are of practical and theoretical interest. Because of the low speed of propagation of ultrasonic waves and pronounced piezoelectric effect, single crystals of sillenites can be used as delay lines, resonators, and surface-wave amplifiers.[3] High photosensitivity, together with the electrooptical effect, allows one to use them in space−time light modulators as well as for recording and reproducing phase holograms with a sensitivity comparable to that of high-resolution photoplates. Some properties of sillenites (e.g., piezoelectric effect and optical activity) depend heavily on the composition (specifically the composition of each crystallographic site of the structure),[2] which usually differs from the nominal composition and the formal charge (FC) of a component (components) occupying the tetrahedral site.

Analysis of the currently available results of the studies of the $Bi^{3+}{}_{24}M_2O_{40}$ (M = Bi, Si, Ge, Mn) phases (Table 1) allows the following conclusions:

1 The defective $Bi^{3+}{}_{24}(Si^{4+}{}_{1.74(6)}\square_{0.26})O_{40-\delta}$ phase ($\square$ is a vacancy)[4] and the defect-free $Bi^{3+}{}_{24}Si^{4+}{}_{1.99(6)}O_{40}$ phase[5] have close unit cell parameters, whereas the

*To whom correspondence should be addressed. E-mail: melti@list.ru.

(1) Sillen, L. G. *Ark. Kemi, Mineral. Geol.* **1937**, Series A12, *18*, 1.
(2) Kargin, Yu. F.; Burkov, V. I.; Marin, A. A.; Egorisheva, A. V. *Moscow*, **2004**.
(3) Radaev, S. F.; Simonov, V. I. *Kristallografiya* **1992**, *37*, 914.
(4) Abrahams, S. C.; Bernstein, J. L.; Svensson, C. *J. Chem. Phys.* **1979**, *71* (2), 788.

Published on Web 02/14/2011

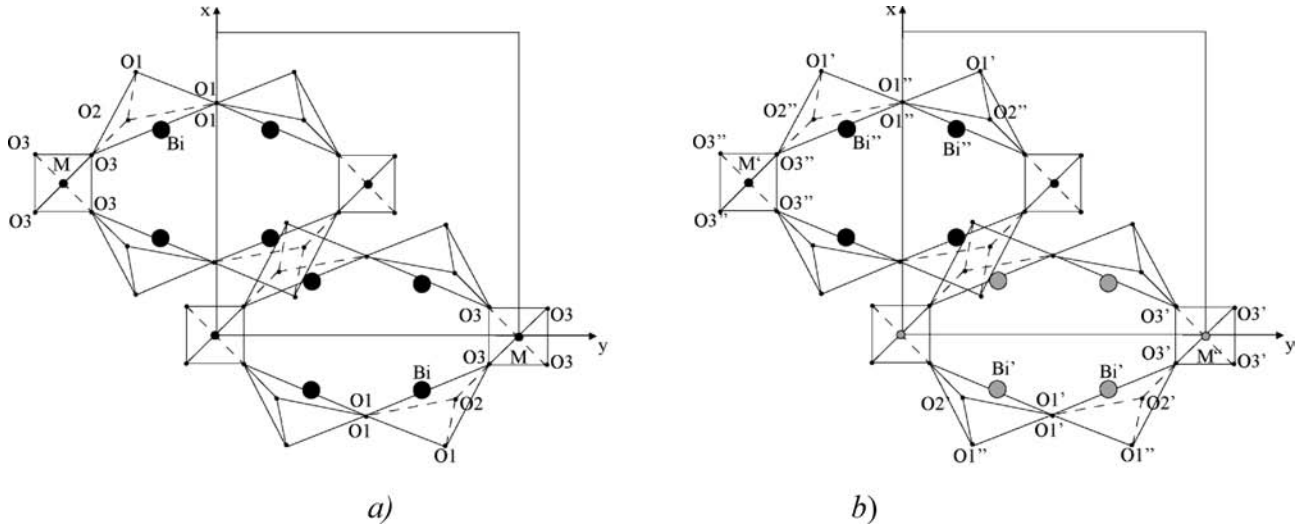

Figure 1. Fragment of the $Bi_{24}M_2O_{40}$ structure in space groups (a) $I23$ and (b) $P23$.

Table 1. Selected Parameters of Sillenites of the $Bi^{3+}{}_{24}M_2O_{40}$ Composition (M = Si, Ge, Mn)

phase	unit cell parameter a, Å	diffraction method	additional methods
$Bi_{24}(Bi^{3+}Bi^{5+})O_{40}$[8]	10.25		
$Bi_{24}(Bi^{3+}{}_{1.60}\square_{0.40})(O_{38.40}\square_{1.60})$[3]	10.2501(1)	neutron diffraction (powder)	
$Bi_{24}(Bi^{3+}{}_2)(O_{39.0}[]_{1.0})$[7]	10.268(1)	X-ray and neutron diffraction (powder)	
$Bi^{3+}{}_{24}Si^{4+}{}_{1.99(6)}O_{40}$[5]	10.104(1)	neutron diffraction (single crystal)	
$Bi^{3+}{}_{24}(Si^{4+}{}_{1.74(6)}[]_{0.26})O_{40-\delta}$[4]	10.10433(5)	X-ray diffraction (single crystal)	
$Bi_{24}Ge^{4+}{}_{2.00(6)}O_{40}$[3]	10.153(4)	neutron diffraction (single crystal)	
$Bi_{24}Ge^{4+}{}_{2.0(1)}O_{40}$[3]	10.148(3)	X-ray diffraction (single crystal)	
$Bi_{24}(Ge^{4+}{}_{1.74(4)}[]_{0.26})O_{40-\delta}$[6]	10.146(1)	X-ray diffraction (single crystal)	
$Bi_{24}[(Bi^{5+}{}_{0.65}Bi^{3+}{}_{0.35})_{0.53}Mn^{3+}{}_{0.47}]_2(O_{39.4}[]_{0.6})$[5]	10.153(1)	neutron diffraction (single crystal)	
$Bi_{24}Mn^{4+}{}_2O_{40}$[9]	10.206(1)	X-ray diffraction (single crystal)	elemental analysis, IR spectroscopy, absorption spectroscopy
$Bi_{24}(Mn^{4+}, Mn^{5+})_2O_{40}$[a,2]	10.216		absorption spectroscopy
$Bi_{24}(Si^{4+},Mn^{4+},Mn^{5+})_2O_{40}$[a,2]			absorption spectroscopy

[a] The nominal composition.

parameters of the defective $Bi_{24}(Ge^{4+}{}_{1.74(4)}\square_{0.26})O_{40-\delta}$ phase[6] and the defect-free $Bi_{24}Ge^{4+}{}_{2.0(1)}O_{40}$[3] and $Bi_{24}Ge^{4+}{}_{2.00(6)}O_{40}$[3] phases are slightly different.

2 The phases with the unit cell parameter a = 10.2501(1) and 10.268(1) Å correspond to the $Bi^{3+}{}_{24}(Bi^{3+}{}_{1.60}\square_{0.40})(O_{38.40}\square_{1.60})$[3] and $Bi^{3+}{}_{24}Bi^{3+}{}_2(O_{39.0}\square_{1.0})$[7] compositions, respectively; that is, they contain vacancies at the tetrahedral positions but not at the cationic positions. Opinions on the FC of the Bi atom at the tetrahedral site differ: both 5+ and 3+[8] or 3+ only.[2,6] However, neither of the two standpoints has received convincing support in experiments.

3 For a single crystal of the $Bi_{24}Mn_2O_{40}$ nominal composition (a = 10.153(1) Å), which was obtained from a solution in a melt of excess Bi_2O_3,[5] determination of the occupancies of the mixed tetrahedral position, followed by their correction based on calculation of the FCs of the Bi and Mn atoms with due regard for the electrical neutrality of the compound, resulted in the $Bi^{3+}{}_{24}[(Bi^{5+}{}_{0.65}Bi^{3+}{}_{0.35})_{0.53}Mn^{3+}{}_{0.47}]_2(O_{39.4}\square_{0.6})$ crystal−chemical formula. According to the data of X-ray crystallography, chemical analysis, IR spectroscopy, and X-ray absorption spectroscopy, dark-green cubic single crystals of the $Bi_{24}Mn_2O_{40}$ nominal composition (a = 10.206(1) Å)[9] that were grown by the hydrothermal method do not contain vacancies and their crystal−chemical formula is represented as $Bi^{3+}{}_{24}Mn^{4+}{}_2O_{40}$. On the contrary, the absorption spectra of $Bi_{24}Mn_2O_{40}$ crystals (a = 10.216 Å) studied in ref [2] revealed comparable contents of Mn^{4+} and Mn^{5+} ions (the same situation was observed for $Bi_{24}Si_2O_{40}$:Mn crystals).

Thus, both defective and defect-free sillenite phases have been obtained in the $Bi_2O_3-SiO_2-MnO_2$ system. They differ in the unit cell parameters a and FCs of the cations, and the a parameters do not correlate with unit cell compositions. In most cases, the compositions of the specimens obtained are in conflict with the electrical neutrality and differ from the starting batch composition.

(5) Neov, S.; Marinova, V.; Reehuis, M.; et al. *Appl. Phys.* **2002**, *A74*, S1016.
(6) Svensson, C.; Abrahams, S. C.; Bernstein, J. L. *Acta Crystallogr.* **1979**, *B35*, 2687.
(7) Harwig, H. A. *Z. Anorg. Allg. Chem.* **1978**, *444*, 151.
(8) Craig, D. C.; Stephenson, N. C. *J. Solid State Chem.* **1975**, *15*, 1.
(9) Delicat, U.; Radaev, S. F.; Tromel, M.; et al. *J. Solid State Chem.* **1994**, *110*, 66.

Table 2. Compositions and Selected Crystal−Chemical Parameters of the Specimens Studied

specimen	no.	starting batch composition	crystal−chemical formula; R; D, %; FC_{calcd}/FC_{exp}	space group	morphology	unit cell parameter a, Å
powdered single crystals	1	$NaBiO_3 + SiO_2$	$Bi_{24}Si^{4+}_{2.00(4)}O_{40}$; $R_p = 5.15$, $R_{wp} = 6.54$; $D = 3.6$	$I23$[a]	cube	10.1041(4)
	2	$NaBiO_3 + GeO_2$	$Bi_{24}Ge^{4+}_2O_{40}$; $R_p = 7.47$, $R_{wp} = 9.51$; $D = 4.3$	$I23$[a]	cube	10.1452(1)
	3	$NaBiO_3 + MnCl_2 \cdot 4H_2O$	$Bi_{24}(Bi^{3+}_{0.94(4)}Mn^{4+}_{1.06})(O_{39.50}\square_{0.50})$; $R_p = 11.44$, $R_{wp} = 14.37$; $D = 6.5$	$I23$[a]	cube	10.2139(4)
	4	$NaBiO_3 + Na_2SiO_3 \cdot 9H_2O + Mn(NO_3)_2 \cdot 6H_2O$	$Bi_{24}(Si^{4+}_{1..32(4)}Mn^{4+}_{0.68})O_{40}$; $R_p = 4.79$, $R_{wp} = 6.28$; $D = 4.5$	$I23$[a]	epitaxial film	10.1025(2)
	5	$NaBiO_3 + Na_2SiO_3 \cdot 9H_2O + Mn(NO_3)_2 \cdot 6H_2O$	$Bi_{24}(Si^{4+}_{1.16(4)}Mn^{4+}_{0.84})O_{40}$; $R_p = 9.38$, $R_{wp} = 12.40$; $D = 3.9$	$I23$[a]	epitaxial film	10.1077(3)
	6	$NaBiO_3 + Na_2SiO_3 \cdot 9H_2O + Mn(NO_3)_2 \cdot 6H_2O$	$Bi_{24}(Si^{4+}_{1.60}Bi^{3+}_{0.30}Mn^{4+}_{0.10})(O_{39.85}\square_{0.15})$; $R_p = 6.18$, $R_{wp} = 8.00$; $D = 4.2$	$I23$[a]	cube	10.1476(3)
single crystals	7	$NaBiO_3 + SiO_2$	$Bi_{24}(Si^{4+}_{1.48(4)}\square_{0.52})(O_{38.96(3)}\square_{1.04})$; $R_1 = 4.49$, $wR_2 = 4.62$; $D = 3.7$	$I23$	cube	10.07723(8)
	8	$NaBiO_3 + MnCl_2 \cdot 4H_2O$	$Bi_{24}(Mn^{4+}_{0.80(4)}\square_{1.20})(O_{37.63(3)}\square_{2.37})$; $R_1 = 9.70$, $wR_2 = 10.18$; $D = 4.2$	$I23$[b]	cube	10.1014(1)
	9	$NaBiO_3 + Na_2SiO_3 \cdot 9H_2O + Mn(NO_3)_2 \cdot 6H_2O$	$Bi_{24}(Si^{4+}_{0.04(8)}Bi^{3+}_{0.60}Mn^{4+}_{1.36})(O_{39.70}\square_{0.30})$; $R_1 = 4.00$, $wR_2 = 4.55$; $D = 4.5$; $FC_{calcd}/FC_{exp} = 3.7(2)/3.7$	$P23$	tetrahedron	10.1866(2)
	10	$NaBiO_3 + Na_2SiO_3 \cdot 9H_2O + Mn(NO_3)_2 \cdot 6H_2O$	$Bi_{24}(Si^{4+}_{1.70(10)}Bi^{3+}_{0.10}Mn^{4+}_{0.20})(O_{39.95(2)}\square_{0.05})$; $R_1 = 11.04$, $wR_2 = 30.64$; $D = 3.9$; $FC_{calcd}/FC_{exp} = 3.3(6)/3.95$	$I23$[b]	tetrahedron	10.138(3)
	11	$NaBiO_3 + Na_2SiO_3 \cdot 9H_2O + Mn(NO_3)_2 \cdot 6H_2O$	$Bi_{24}(Si^{4+}_{1.1(1)}Bi^{3+}_{0.1}Mn^{4+}_{0.8})(O_{39.95}\square_{0.05})$; $R_1 = 3.74$, $wR_2 = 3.95$; $D = 3.5$; $FC_{calcd}/FC_{exp} = 3.5(3)/3.95$	$I23$	tetrahedron−cube combination	10.1456(1)
	12	$NaBiO_3 + Na_2SiO_3 \cdot 9H_2O + Mn(NO_3)_2 \cdot 6H_2O$	$Bi_{24}(Si^{4+}_{0.9(1)}Mn^{4+}_{1.1})O_{40}$; $R_1 = 4.13$, $wR_2 = 4.52$; $D = 3.6$; $FC_{calcd}/FC_{exp} = 4.2(1)/4$	$P23$	cube	10.1287(1)
	13	$NaBiO_3 + Na_2SiO_3 \cdot 9H_2O + Mn(NO_3)_2 \cdot 6H_2O$	$Bi_{24}(Si^{4+}_{0.17(1)}Bi^{3+}_{0.01}Mn^{4+}_{1.82})(O_{39.93(5)}\square_{0.07})$; $R_1 = 3.84$, $wR_2 = 4.13$; $D = 3.6$; $FC_{calcd}/FC_{exp} = 4.2(2)/3.995$	$P23$	cube	10.1504(1)
	14	$NaBiO_3 + Na_2SiO_3 \cdot 9H_2O + Mn(NO_3)_2 \cdot 6H_2O$	$Bi_{24}(Si^{4+}_{0.58(12)}Bi^{3+}_{0.02}Mn^{4+}_{1.40})(O_{39.99}\square_{0.01})$; $R_1 = 5.75$, $wR_2 = 5.27$; $D = 4.7$; $FC_{calcd}/FC_{exp} = 4.0(4)/3.99$	$I23$	tetrahedron−cube combination	10.1510(1)

[a] No reflections violating space group $I23$ were found. [b] The data were not analyzed for violation of the I centering.

The purpose of the work is to determine the composition of sillenites in the $Bi_2O_3-SiO_2-MnO_2$ system and to study their specific structural features.

Experimental Methods

Synthesis. Single crystals of spontaneous nucleation 30−3000 μm in size, whose nominal compositions are $Bi_{24}M_2O_{40}$ (M = Si, Ge, Mn) and $Bi_{24}(Si_{1-x}Mn_x)_2O_{40}$, and epitaxial films of the $Bi_{24}(Si_{1-x}Mn_x)_2O_{40}$ nominal composition were obtained under hydrothermal conditions. The synthesis was performed by the thermal gradient method in autoclaves, 300 mL in volume, lined with fluoroplastic-4 contact inserts at 310 °C, a temperature gradient of 40 °C, and a pressure of 500 kg/cm^2. The starting batch was prepared by thorough stirring of $NaBiO_3$ with SiO_2, GeO_2, or $MnCl_2 \cdot 4H_2O$ for synthesis of the $Bi_{24}M_2O_{40}$ phases with M = Si, Ge, or Mn, respectively, or a mixture of $NaBiO_3$, $Na_2SiO_3 \cdot 9H_2O$, and $Mn(NO_3)_2 \cdot 6H_2O$ for synthesis of the $Bi_{24}(Si_{1-x}Mn_x)_2O_{40}$ phase. An aqueous solution of NaOH (up to 30 wt %) was used as a solvent. Plates of $Bi_{24}Si_2O_{40}$, ~50 × 20 × 3 mm in size, prepared by the Czochralski method (Bi_2O_3:SiO_2 = 6:1, t = 920 ± 10 °C, platinum crucible, growth rate 2 mm/h) were used as substrates for epitaxial growth. The specimens obtained are listed in Table 2.

In the course of hydrothermal synthesis, the concentration of the batch components in the alkaline solution decreases and the rate of crystal growth increases; therefore, it is highly probable that single crystals of spontaneous nucleation will have different compositions deviating from the nominal composition.

Diffraction and Spectroscopic Study. Single-crystal X-ray diffraction studies of $Bi_{24}Si_2O_{40}$ (specimen 7), $Bi_{24}Mn_2O_{40}$ (specimen 8), and $Bi_{24}(Si_{1-x}Mn_x)_2O_{40}$ (specimens 9−14) were carried out at room temperature on an Xcalibur S diffractometer equipped with a two-dimensional CCD detector (Oxford Diffraction) or a CAD-4 diffractometer with a point detector. The coordinates and anisotropic thermal parameters of all atoms, as well as the site occupancies of the cations and all O atoms, were refined using the *JANA2000*[10] and *SHELXL97*[11] programs.

In order to avoid correlations between occupancies and thermal parameters of the atoms that occupy the tetrahedral site, the refinement was performed by the following stages: (1) the occupancy of the tetrahedral site populated by an M atom in the $Bi_{24}M_2O_{40}$ compounds or shared by Si and Mn atoms in the $Bi_{24}(Si_{1-x}Mn_x)_2O_{40}$ solid solutions starting with different ratios (Si > Mn, Si < Mn, and Si = Mn); (2) the thermal parameters together with the site occupancy of the M (Si and Mn) atoms with all other parameters fixed; (3) the thermal parameters of all atoms and the occupancy of the tetrahedral site. A facility of *SHELXL97* to refine three atoms (Bi, Si, and Mn) located at a mixed position was used for specimens 9−11, 13, and 14.

The X-ray diffraction patterns of powdered single crystals $Bi_{24}M_2O_{40}$ with M = Si, Ge, or Mn (specimens 1−3) and $Bi_{24}(Si_{1-x}Mn_x)_2O_{40}$ (specimen 6), as well as those of $Bi_{24}(Si_{1-x}Mn_x)_2O_{40}$

(10) Dusek, M.; Petricek, V.; Wunschel, M.; et al. *J. Appl. Crystallogr.* **2001**, *34*, 398.
(11) Sheldrick, G. M. *Acta Crystallogr.* **2008**, *A64*, 112.

epitaxial films, which were detached from substrates (specimens 4 and 5), were recorded on an HZG-4 diffractometer (Cu Kα, Ni filter, reflection geometry). The data were collected for rotating specimens in a stepwise mode (scanning in 0.02° steps at 15 s pulse storage time in the 2θ range 10−100°). In order to identify the phases formed and unreacted starting components, the X-ray phase analysis was performed using the PCPDFWIN PDF2 automated database. No outliers that could be identified with impurities or violate space group $I23$ were found among the diffraction reflections. The unit cell parameters were refined using the *DICVOL04* program[12] (Table 2).

All calculations related to the refinement of the composition and structure of the powdered single crystals and polycrystalline specimens were performed by the full-profile Rietveld method using the *DBWS-9411*[13] and *FullProf Suite*[14] program packages. The peak shape was characterized by the pseudo-Voigt function at 8.0 fwhm, where fwhm is a half-width of a peak. The stage of the refinement of the overall scale factor, background level, counter zero point, and specimen displacement was followed by the refinement of the profile and structural parameters together with the background level. The structural parameters were refined in the following steps: at first, only the coordinates of all atoms; the thermal parameters of all atoms in the isotropic and then anisotropic approximation at fixed positional parameters and site occupancies; the site occupancy at fixed coordinates and thermal parameters for each atomic position; and finally, the thermal parameters together with the site occupancy for each atomic position.

In structure 6, the occupancies of the Si, Mn, and Bi atoms sharing the tetrahedral site could not be refined within the *DBWS-9411* and *FullProf Suite* programs. The occupancies of these atoms were estimated by variation of their ratio and comparison of the corresponding isotropic thermal parameters with those determined in the single-crystal experiment. For specimens 3, 6, 9, 11, and 14, the refinement of the occupancies of the O positions failed; therefore, these occupancies were calculated with due regard for the electrical neutrality of the system.

IR spectra of powdered epitaxial films of $Bi_{24}(Si_{1-x}Mn_x)_2O_{40}$ (specimens 4 and 5) were recorded on a Bruker Equinox 55 Fourier spectrometer (ν = 400−1000 cm^{-1}).

Bond-Valence Method. The validity of the structural data was verified by calculation of the local valence balance within two approaches of the bond-valence method:

1 The validity of the crystal structure determination was estimated within the method of Pyatenko, who proposed the D criterion [$D = \sum|\Delta|/\sum v_a$]; $|\Delta| = |\sum v_i - v_a|$, where v_i is a valence strength and v_a is the FC of an anion), which should be < 5%.[15] In the calculation of the polyhedron constant $k_i = v_c/[\sum_i 1/r_i^n]$ (v_c is the FC of a cation at the tetrahedral site and r_i is the experimental value of the interatomic distance between a cation and anions), the value n(Bi) = 4.5 determined earlier[16] was used.

2 The FC of a cation at the tetrahedral site (FC_{calcd}) was calculated as described in ref 17: $z_j = \sum S_{ij}$, where z_j is the FC (valence) of a cation and $S_{ij} = \exp[(R_{ij} - d_{ij})/0.37]$ is the valence of a bond between a cation and an anion [R_{ij} is the M−O or (M′,M″)−O distance corresponding to the valence strength equal to unity and d_{ij} is the experimental M−O or (M′,M″)−O distance].

The minimal R factors and the D values calculated using the bond-valence method served as criteria for the validity of the structure refinement and composition determination. In addition, the atomic thermal parameters and interatomic distances were analyzed in comparison with the literature data.

Results

The unit cell parameters, atomic coordinates, equivalent isotropic thermal parameters $U_{eq}\times10^2$ (Å^2), site occupancies μ, and selected interatomic distances d (Å) for powdered and single crystals are listed in Tables 3 and 4, respectively. The phase compositions, R factors, D values, and FCs of cations at the mixed M position are summarized in Table 2.

When determining the occupancy of the tetrahedral site, we assumed that the FCs of the Bi and Mn ions were 3+ and 4+, respectively, as was found in the previous studies.

Bi_2O_3−$M^{4+}O_2$ System. The refinement of the crystal structure of powdered single crystals of the $Bi_{24}M^{4+}{}_2O_{40}$ (M^{4+} = Si, Ge) nominal composition showed that the Bi1, M, and O positions are free of defects (within experimental error). The thermal parameters ($U_{eq} \times 10^2 \sim 0.4-0.6$ Å^2) close to those determined for the phase with M = Ge ($U_{eq} \times 10^2 = 0.51(2)$ Å^2)[3] and minimal R factors were obtained for the stoichiometric $Bi_{24}M^{4+}{}_2O_{40}$ compositions (Table 2, specimens 1 and 2).

The refinement of the site occupancies of O atoms in the structure of a powdered specimen of the $Bi_{24}Mn^{4+}{}_2O_{40}$ nominal composition (a = 10.2139(4) Å, specimen 3) resulted in a decreased thermal parameter of the Mn atom, $U_{eq}\times10^2 \sim 0.05$ Å^2. The introduction of a heavy Bi atom into this site increased the thermal parameter to a reasonable value of $U_{eq} \times 10^2 = 0.46(7)$ Å^2, decreased the R factor, and resulted in the electrically neutral formula $Bi_{24}(Bi^{3+}{}_{0.94(4)}Mn^{4+}{}_{1.06})(O_{39.50}\square_{0.50})$ (Table 3). Note that Bi ions were found at the M tetrahedral site in crystals of the $Bi_{24}(V^{5+}{}_{1.78}Bi^{3+}{}_{0.06}\square_{0.16})O_{40.54}$[3] and $Bi_{24}[(V^{5+}O_4)(Bi^{3+}O_4)]O_{32}$[18] phases.

The unit cell parameters of single crystals of the $Bi_{24}Si^{4+}{}_2O_{40}$ and $Bi_{24}Mn^{4+}{}_2O_{40}$ nominal compositions [specimens 7 and 8; a = 10.07723(8) and 10.1014(1) Å, respectively] are smaller than those of the specimens having the same nominal compositions, which were reported in refs [5] and [9] or prepared in this study [$Bi_{24}Si^{4+}{}_2O_{40}$, specimen 1, a = 10.1041(4) Å; $Bi_{24}Mn^{4+}{}_2O_{40}$, specimen 3, a = 10.2139(4) Å]. The structural study of specimens 7 and 8 revealed a large number of vacancies at the M = Si, Mn, and O atomic positions. The compositions of phases 7 and 8 can be written as $Bi_{24}(Si^{4+}{}_{1.48(4)}\square_{0.52})(O_{38.96(3)}\square_{1.04})$ and $Bi_{24}(Mn^{4+}{}_{0.80(4)}\square_{1.20})(O_{37.63(3)}\square_{2.37})$, respectively. Analysis of the residual electron density revealed peaks >0.19 e/Å^3 with coordinates x = 0.016, y = 0.32, z = 0.17 (a 24f site) close to the coordinates of Bi1 (x = 0.17, y = 0.019, z = 0.31). This peak is indicative of a structural disordering due to a pronounced defect at the tetrahedral site.

Bi_2O_3−SiO_2−MnO_2 System. In the course of spontaneous crystallization under hydrothermal conditions in the Bi_2O_3−SiO_2−MnO_2 system, single crystals in the shape of a cube, tetrahedron, and a combination of a cube and a tetrahedron were obtained (Figure 2).

(12) Boultif, A.; Louër, D. *J. Appl. Crystallogr.* **2004**, *37*, 724.
(13) Young, R. A.; Sakthivel, A.; Moss, T. S. et al. *User's guide to program DBWS-9411*; High Pressure Research Centre UNIPRESS: Warsaw, Poland, 1995.
(14) Rodriguez-Carvajal, J. *An introduction to the program FullProf 2000*; Laboratoire Leon Brillouin: (CEA-CNRS) CEA/Saclay, France, 2001.
(15) Pyatenko, Yu. A. *Kristallografiya* **1972**, *17*, 773.
(16) Kuz'micheva, G. M.; Mel'nikova, T. I. *Russ. J. Inorg. Chem.* **2009**, *54* (1), 74.
(17) Brown, I. D.; Altermatt, D. *Acta Crystallogr.* **1985**, *B 41*, 244–247.
(18) Yudin, A. N.; Pobedimskaya, E. A.; Terent'eva, L. E.; et al. *Inorg. Mater.* **1989**, *25*(10), 1715.

Table 3. Atomic Coordinates, Equivalent Isotropic Thermal Parameters $U_{eq} \times 10^2$ (Å^2), Site Occupancies μ, and Selected Interatomic Distances d (Å) for Powdered Single Crystals

	no.					
parameter	1	2	3	4	5	6
unit cell parameter a, Å	10.1041(4)	10.1452(1)	10.2139(4)	10.1025(2)	10.1077(3)	10.1476(3)
Bi1						
x	0.1758(1)	0.1759(1)	0.1775(2)	0.1759(1)	0.1753(1)	0.1758(2)
y	0.3174(1)	0.3181(1)	0.3206(1)	0.3174(1)	0.3173(0)	0.3192(1)
z	0.0162(1)	0.0170(1)	0.0213(1)	0.0159(1)	0.0166(0)	0.0166(1)
μ	1.0	1.0	1.0	1.0	1.0	1.0
$U_{eq} \times 10^2$	0.50(3)	0.51(1)	0.52(1)	0.49(2)	0.53(3)	0.51(1)
M						
μ	Si = 1.00(2)	Ge = 1.00	Bi = 0.47(2) Mn = 0.53(2)	Si = 0.66(2) Mn = 0.34(2)	Si = 0.58(2) Mn = 0.42(2)	Si = 0.80[a] Bi = 0.15[a] Mn = 0.05[a]
$U_{eq} \times 10^2$	0.53(11)	0.41(12)	0.46(7)	0.54(8)	0.47(6)	0.43(6)
O1						
x	0.1349(6)	0.1333(7)	0.1362(12)	0.1348(6)	0.1318(5)	0.1331(3)
y	0.2551(6)	0.2604(8)	0.2751(13)	0.2554(6)	0.2600(6)	0.2460 (5)
z	0.488(1)	0.4910(8)	0.5041(20)	0.4885(13)	0.4959(12)	0.4889(11)
μ	1.0	1.0	1.0	1.0	1.0	1.0
$U_{eq} \times 10^2$	0.9(2)	0.96(14)	1.02(12)	1.0(3)	1.2(3)	0.9(4)
O2						
x	0.1969(6)	0.1922(7)	0.2046(11)	0.1982(6)	0.1954(7)	0.2018(8)
μ	1.0	1.0	1.0	1.0	1.0	1.0
$U_{eq} \times 10^2$	0.9(1)	1.02(12)	1.1(2)	0.8(4)	1.1(2)	0.7(4)
O3						
x	0.9067(8)	0.901(1)	0.8986(9)	0.9058(9)	0.9055(7)	0.9045(11)
μ	1.0	1.0	0.937[b]	1.0	1.0	0.981[b]
$U_{eq} \times 10^2$	0.96(15)	0.85(16)	1.3(1)	1.2(3)	0.9(3)	0.8(4)
Bi1−×O1	2.068(5)	2.110(5)	2.146(7)	2.067(5)	2.109(6)	2.069(5)
Bi1−×O1	2.247(12)	2.281(10)	2.426(25)	2.253(14)	2.313(15)	2.206(13)
Bi1−×O1	2.615(2)	2.610(2)	2.605(3)	2.609(5)	2.560(3)	2.570(4)
Bi1−×O2	2.205(2)	2.195(2)	2.233(4)	2.212(2)	2.196(3)	2.241(3)
Bi1−×O3	2.640(22)	2.633(12)	2.618(12)	2.646(9)	2.645(5)	2.667(4)
$[Bi-O]_{av}$	2.358(3)	2.366(6)	2.40(4)	2.358(3)	2.365(3)	2.351(6)
(Bi2,Si,Mn)−4× O3	1.633(14)	1.740(16)	1.794(29)	1.648(15)	1.655(12)	1.679(11)

[a] The parameter was not refined. [b] The site occupancy was calculated with due regard for the electrical neutrality of the system.

We found that the morphology of $Bi_{24}(Si_{1-x}Mn_x)_2O_{40}$ crystals depends on the batch composition. Cubic crystals are formed in the systems with a molar ratio of the starting components $Na_2SiO_3 \cdot 9H_2O$:$Mn(NO_3)_2 \cdot 6H_2O$ > 1. Tetrahedral crystals are formed at the reverse molar ratio, that is, $Na_2SiO_3 \cdot 9H_2O$:$Mn(NO_3)_2 \cdot 6H_2O$ < 1. Combined-shape crystals are obtained in the systems containing equimolar amounts of $Mn(NO_3)_2 \cdot 6H_2O$ and $Na_2SiO_3 \cdot 9H_2O$. Figure 3 shows a concentration triangle for the $NaBiO_3$ + $Na_2SiO_3 \cdot 9H_2O$ + $Mn(NO_3)_2 \cdot 6H_2O$ ternary system, which represents the starting batch composition, with the field of formation of sillenite-type crystals.

The refinement of the structural parameters of solid solutions with the sillenite-type structure led to the following results:

1 In all phases studied, no vacancies were found at the Bi1 position. Vacancies at the O3 positions were found in all phases except 4, 5, and 12 (Tables 3 and 4). The extension of the data obtained for single crystals (specimens 7 and 8) to powders allows one to assert that powders also contain oxygen vacancies.

2 For the $Bi_{24}(Si_{2-x}Mn_x)O_{40}$ phases prepared at different starting compositions (Si = Mn, Si > Mn, and Si < Mn), the refinement of the M site occupancy resulted in x values equal to 1.1 (a = 10.1287 Å, specimen 12), 0.84 (a = 10.1077 Å, specimen 5), and 0.68 (a = 10.1025 Å, specimen 4; Figure 4) (Tables 2−4). For these compositions, the isotropic thermal parameters are close to those found in other sillenites, the interatomic distances have normal lengths, the FCs of the M atoms coincide with the values calculated by the bond-valence method, and the R factor and D have the minimal values. In these phases, oxygen vacancies are absent and the unit cell parameter decreases with the mean radius of the M atom ($r_{Si^{4+}}$ = 0.26 Å; $r_{Mn^{4+}}$ = 0.39 Å).

3 For specimens 6, 9−11, 13, and 14, similar indications of the validity are achieved under the condition that, in addition to the Si and Mn ions, Bi ions enter into the M tetrahedral sites 2−4).

Analysis of the sets of diffraction reflections for specimens 9, 12, and 13 (Table 2) revealed a number of reflections whose indices violate the I centering (hkl, $h + k + l \neq 2n$; $0kl$, $k + l \neq 2n$; hhl, $l \neq 2n$; $h00$, $h \neq 2n$) but fit space group $P23$. Such extra reflections for sillenite-type crystals had not been observed earlier and were not found for specimens 7, 11, and 14 (Table 2). The crystal−chemical formula of specimen 13, which was calculated by the *SHELXL97* program, can be represented as $Bi_{24}(Si^{4+}_{0.17(1)}Bi^{3+}_{0.01}Mn^{4+}_{1.82})(O_{39.93(5)}\square_{0.07})$ (space group $I23$; Figure 1a) or $Bi_{24}(Bi_{0.04(2)}Si_{0.05}Mn_{0.91})$-$(Bi_{0.08(2)}Si_{0.30}Mn_{0.62})(O_{39.93(5)}\square_{0.07})$ (space group $P23$; Figure 1b); that is, in going from space group $I23$ to $P23$, the crystallographic positions of the atoms split; for example, the

Table 4. Unit Cell Parameters, Atomic Coordinates, Equivalent Isotropic Thermal Parameters $U_{eq} \times 10^2$ (Å^2), Site Occupancies μ, and Selected Interatomic Distances d (Å) for Single Crystals[a]

	no.							
parameter	7	8	9	10	11	12	13	14
unit cell parameter a, Å	10.07723(8)	10.1014(1)	10.1866(2)	10.138(3)	10.1456(1)	10.1287(1)	10.1432(21)	10.1510(1)
Bi1								
x	0.17565(5)[b]	0.173(2)[b]	0.17719(5)[b]	0.82321(8)	0.17683(3)[b]	0.17664(4)[b]	0.31919(1)	0.17729(5)[b]
y	0.31748(6)	0.020(2)	0.32060(6)	0.98153(8)	0.31960(4)	0.31919(5)	−0.01883(1)	0.32027(6)
z	0.01579(5)	0.314(2)	0.01774(5)	0.68064(8)	0.01915(4)	0.01872(5)	−0.17671(1)	0.01964(6)
μ	1.0	1.0	1.0	1.0	1.0	1.0		1.0
$U_{eq} \times 10^2$	0.84(1)	1.42(6)	1.47(14)	1.037(15)	1.364(7)	0.724(8)	0.830(2)	1.3(1)
Bi2 μ			0.30(4)	0.05(7)	0.05(5)		0.006(2)	0.01(6)
Si μ	0.74(2)		0.02(4)	0.83(7)	0.55(5)	0.47(7)	0.084(2)	0.29(6)
Mn μ		0.40(2)	0.68(4)	0.1(7)	0.40(5)	0.53(7)	0.910(2)	0.70(6)
$U_{eq} \times 10^2$	0.8(1)	0.9(5)	0.49(1)	0.9(3)	0.64(4)	0.7(2)	0.99(19)	0.90(6)
O1								
x	0.1337(13)	0.364(3)	0.1352(12)	0.365(2)	0.1336(9)	0.135(1)	0.2553(3)	0.1379(11)
y	0.2517(13)	0.978(3)	0.2493(11)	0.009(2)	0.2492(8)	0.2511(9)	0.0102(3)	0.2520(10)
z	0.4849(12)	0.257(3)	0.4895(12)	0.247(2)	0.4890(9)	0.487(1)	−0.3694(3)	0.4854(13)
μ	1.0	1.0	1.0	1.0	1.0	1.0	1.0	1.0
$U_{eq} \times 10^2$	1.1(2)	1.8(2)	1.8(3)	0.9(2)	1.7(2)	1.1(1)	2.13(7)	1.4(2)
O2								
x	0.1974(17)	0.205(7)	0.1898(13)	0.803(2)	0.1975(9)	0.1988(9)	0.1977(3)	0.195(4)
μ	1.0	0.91(1)	1.0	1.0	1.0	1.0	1.0	1.0
$U_{eq} \times 10^2$	1.1(2)	1.8(2)	2.2(2)	1.0(4)	1.6(1)	0.8(2)	2.05(9)	1.6(2)
O3								
x	0.903(4)	0.908(6)	0.894(2)	0.098(3)	0.9036(10)	0.905(1)	0.0915(3)	0.902(4)
μ	0.87(1)	0.79(2)	0.963[c]	0.987(5)	0.75[c]	1.0	0.98(1)	0.998[c]
$U_{eq} \times 10^2$	1.3(4)	2.6(4)	2.3(2)	2.3(9)	1.9(1)	1.6(3)	1.1(1)	2.2(2)
Bi1−×O1	2.068(13)	2.05(4)	2.060(12)	2.07(2)	2.069(9)	2.06(1)	2.0805(28)	2.044(11)
Bi1−×O1	2.202(12)	2.15(4)	2.220(12)	2.24 (2)	2.200(9)	2.20(1)	2.1808(30)	2.197(12)
Bi1−×O1	2.612(12)	2.72(4)	2.590(12)	2.59(2)	2.591(9)	2.61(1)	2.5545(30))	2.650(12)
Bi1−×O2	2.205(17)	2.19(8)	2.205(13)	2.205(7)	2.203(9)	2.21 (1)	2. 2036(11)	2.19(4)
Bi1−×O3	2.62(4)	2.64(7)	2.62(2)	2.66(2)	2.677(10)	2.67(1)	2.7081(24)	2.68(4)
$[Bi-O]_{av}$	2.34(19)	2.35(5)	2.34(1)	2.35(2)	2.348(9)	2.35(1)	2.3455(25)	2.35(2)
(Bi2,Si,Mn)−4×O3	1.69(4)	1.61(6)	1.88(2)	1.73(5)	1.694(10)	1.67(1)	1.6071(53)	1.72(4)

[a] The parameter was not refined. [b] Left-handed form of the crystal. [c] The site occupancy was calculated with due regard for the electrical neutrality of the system.

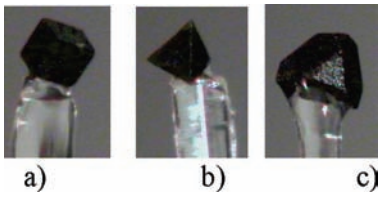

Figure 2. Single crystals in the $Bi_2O_3-SiO_2-MnO_2$ system: cubic faceting (a); tetrahedral faceting (b); a combination of a cube and a tetrahedron (c).

O1′ and O2″ positions in space group $P23$ correspond to the O1 position in space group $I23$ (Figure 1b).[19]

The range $\nu = 850-650$ cm^{-1} of the IR spectra of specimens 4 and 5 is shown in Figure 5. The asymmetry of the band in the range $\nu = 760-840$ cm^{-1} is due to overlap of the bands assigned to the bond vibrations in the $[Si^{4+}O_4]^{4-}$ and $[Mn^{5+}O_4]^{3-}$ tetrahedra, and the band at $\nu = 727$ cm^{-1} is assigned to the vibrations in the $[Mn^{4+}O_4]^{4-}$ tetrahedron.[9] It is impossible to judge the presence of Mn^{3+} ions in sillenites from the IR spectra because the band corresponding to the vibrations of bonds in the $[Mn^{3+}O_4]^{5-}$ tetrahedron should appear in the range $\nu = 530-600$ cm^{-1},[9] which is covered with the band of bond vibrations in the $Bi^{3+}O_5$ semioctahedron ($\nu = 400-660$ cm^{-1}).

Discussion

$Bi_2O_3-M^{4+}O_2$ System. Figure 6 shows a plot of the unit cell parameters a of the $Bi_{24}M^{4+}{}_2O_{40}$ phase against the radii of the tetrahedral M^{4+} cations. The straight line passes through the dots corresponding to the defect-free phases $Bi_{24}Si^{4+}{}_{2.00(4)}O_{40}$ (1) and $Bi_{24}Ge^{4+}{}_2O_{40}$ (2) (Tables 2 and 3) (according to ref [3], the radius of the Ge^{4+} ion is optimal for a sillenite-type structure and phases with M^{4+} = Si or Ge are said to be ideal sillenites). The dots corresponding to the $Bi_{24}Mn^{4+}{}_2O_{40}$ phase studied in ref [9] and the $Bi_{24}(Bi^{3+}{}_{0.94(4)}Mn^{4+}{}_{1.06})(O_{39.5}\square_{0.5})$ phase determined in this study (3) deviate upward from the line (the radius of the M^{4+} cation was calculated as the mean radius of cations sharing the tetrahedral site), whereas the dots corresponding to phases $Bi_{24}(Si^{4+}{}_{1.48(4)}\square_{0.52})(O_{38.96(3)}\square_{1.04})$ (7) and $Bi_{24}(Mn^{4+}{}_{0.80(4)}\square_{1.20})(O_{37.63(3)}\square_{2.37})$ (8) deviate downward. The increase in the a parameter in the former compounds is probably due to the presence of Bi ions ($r_{Bi} > r_M$) at the M tetrahedral site, as is found for specimen 3, and the decrease in the a parameter in the latter compounds is associated with the vacancies at the M site. The unit cell parameter of the stoichiometric $Bi_{24}Mn^{4+}{}_2O_4$ phase ($r_{Mn^{4+}} = 0.39$ Å[20]) estimated from Figure 6 is $a \sim 10.15$ Å.

$Bi_2O_3-SiO_2-MnO_2$ System. In Figure 7, the unit cell parameters a of the phases in the $(1-x)Bi^{3+}{}_{24}Si^{4+}{}_2O_{40} - x(Bi^{3+}{}_{24}Mn^{4+}{}_2O_{40})$ and $(1-x)Bi^{3+}{}_{24}Bi^{3+}{}_2(O_{39}\square_1) -$

(19) Mel'nikova, T. I.; Kuz'micheva, G. M.; Rybakov, V. B.; et al. *Cryst. Rep.* **2010**, *55*(2), 229.

(20) Shannon, R. D. *Acta Crystallogr., Sect. A* **1976**, *32*(6), 751.

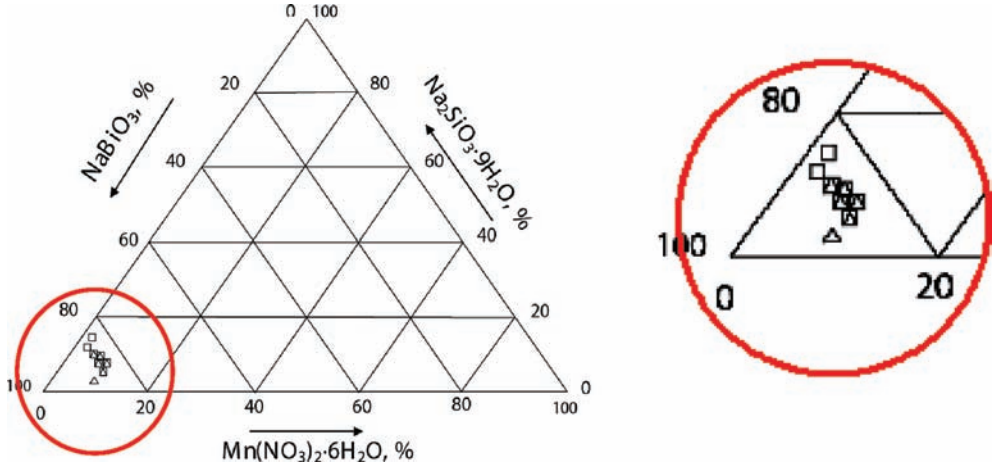

Figure 3. Morphology of sillenite crystals versus batch composition in the $Bi_2O_3-SiO_2-MnO_2$ system (squares for cubic crystals, triangles for tetrahedral crystals, and triangles enclosed in squares for combined-shape crystals).

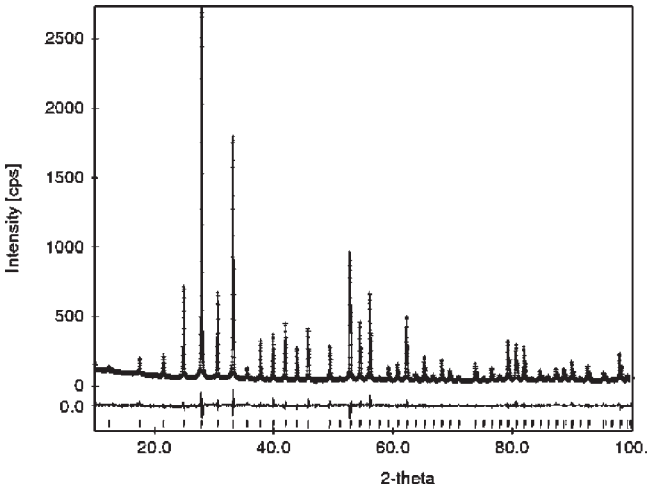

Figure 4. Experimental and calculated X-ray diffraction patterns for specimen 4 ($Bi_{24}(Si^{4+}_{1.32(4)}Mn^{4+}_{0.68})O_{40}$).

$x(Bi^{3+}{}_{24}Mn^{4+}{}_2O_{40})$ systems are plotted against the variable parameter of composition x. On the assumption that a is a linear function of x, straight lines I and II are drawn for the two systems, respectively, based on the data for the stoichiometric $Bi^{3+}{}_{24}Si^{4+}{}_2O_{40}$ phase determined in the experiment (Tables 2 and 3), the data for the $(Bi_{24}Mn^{4+}{}_2O_{40})$ phase estimated using Figure 6, and the data for the $Bi^{3+}{}_{24}Bi^{3+}{}_2(O_{39}\square_1)$ phase reported in ref [7] (Table 1).

A downward deviation of the dots corresponding to powdered epitaxial films $Bi_{24}(Si_{1.32(4)}Mn_{0.68})O_{40}$ (4) and $Bi_{24}(Si_{1.16(4)}Mn_{0.84})O_{40}$ (5) from line I (Figure 7 and Table 2) can be explained by the presence of not only Mn^{4+} ions but Mn^{5+} ions as well ($r_{Mn^{4+}} > r_{Mn^{5+}}$). This conclusion is supported by the IR spectra of phases 4 and 5 (Figure 5a,b). A slight upward deviation of dot 3 from line II is probably due to the presence of an admixture of Mn^{3+} ions ($r_{Mn^{3+}} > r_{Mn^{4+}}$).

Upward deviations of the dots corresponding to crystals $Bi_{24}(Si^{4+}{}_{1.70(10)}Bi^{3+}{}_{0.10}Mn^{4+}{}_{0.20})(O_{39.95(2)}\square_{0.05})$ (10), $Bi_{24}(Si^{4+}{}_{1.1(1)}Bi^{3+}{}_{0.1}Mn^{4+}{}_{0.8})(O_{39.95}\square_{0.05})$ (11), $Bi_{24}(Si^{4+}{}_{0.17(1)}Bi^{3+}{}_{0.01}Mn^{4+}{}_{1.82})(O_{39.93(5)}\square_{0.07})$ (13), and $Bi_{24}(Si^{4+}{}_{0.58(12)}Bi^{3+}{}_{0.02}Mn^{4+}{}_{1.40})(O_{39.99}\square_{0.01})$ (14), as well as to powdered specimens 3 and 6, from line I (Figure 7 and Table 2) are due to the presence of Bi^{3+} ions. The dots corresponding to crystals $Bi_{24}(Si^{4+}{}_{0.9(1)}Mn^{4+}{}_{1.1})O_{40}$ (12) and $Bi_{24}(Si^{4+}{}_{0.04(8)}Bi^{3+}{}_{0.60}Mn^{4+}{}_{1.36})(O_{39.70}\square_{0.30})$ (9) (Table 2) lie in lines I and II, respectively (Figure 7).

As mentioned above, specimens 9, 12, and 13 crystallize in space group $P23$, although these phases are formed in the region of stability of phases crystallizing in space group $I23$. The lowering of symmetry from a body-centered-cubic cell to a primitive cubic cell results from a kinetic phase transition of the order–disorder type,[21,22] which consists of a partial ordering of atoms that occupy defective positions. Analysis of the data available for sillenite-type crystals revealed two factors that determine the feasibility of this kinetic phase transition, namely, specific structural features and growth conditions. A necessary condition for such ordering to occur is the presence of structural positions shared by atoms with different crystal–chemical properties (size, FC, electronegativity, etc.). This condition is met in crystals of the sillenite family. The partial ordering can take place under specific synthesis conditions. According to ref [22], growth dissymmetrization occurs most often in the course of crystallization from solution and under quasi-equilibrium conditions (in our case, growth under hydrothermal conditions). According to our data, the batch composition also affects the ordering of atoms in crystals. Judging by the preliminary data, the symmetry of the crystals correlates with their morphology:

1 Crystals that have a cubic or a tetrahedral faceting were obtained from batches with molar ratios of the starting components $Na_2SiO_3 \cdot 9H_2O$:Mn-$(NO_3)_2 \cdot 6H_2O \neq 1$. These crystals belong to space group $P23$. The lowering of symmetry in these crystals can be explained as follows: the positions that are equivalent in the body of a crystal become inequivalent in the geometry and energy on its surface; as the crystal grows, the inequivalence of the positions is retained because of the low diffusion rate at a low temperature of growth (below 400 °C); that is, the positions split and the symmetry of the crystal lowers.

(21) Chernov, A. A. *Usp. Fiz. Nauk* **1970**, *100*, 277.
(22) Shtukenberg, A. G.; Punin, Yu. O.; Frank-Kameneckaya, O. V. *Usp. Khim.* **2006**, *75*(12), 1212.

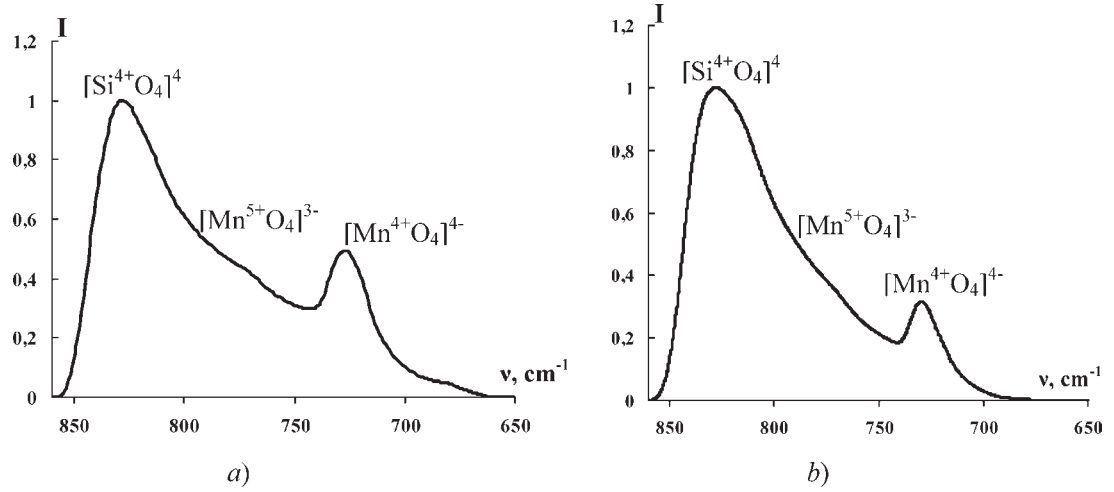

Figure 5. IR spectra of bond vibrations in the $[MO_4]$ tetrahedra in $Bi_{24}(Si_{1-x}Mn_x)_2O_{40}$ sillenites: (a) specimen 4; (b) specimen 5.

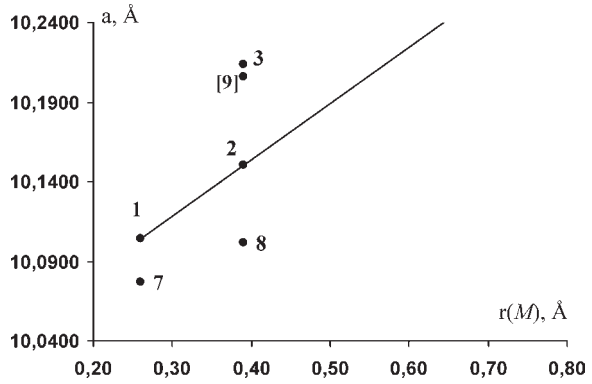

Figure 6. Unit cell parameters versus radii of the M^{4+} cations in sillenites of the $Bi_{24}M^{4+}{}_2O_{40}$ composition.

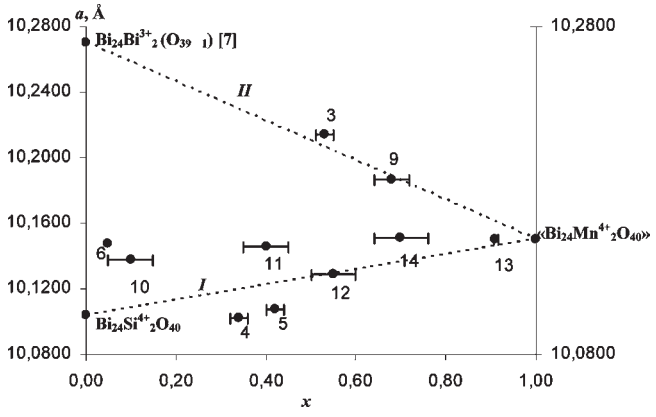

Figure 7. Unit cell parameters a of solid solutions in the $(1 - x)$-$Bi^{3+}{}_{24}Si^{4+}{}_2O_{40} - x(Bi_{24}Mn^{4+}{}_2O_{40})$ (line I) and $(1 - x)Bi^{3+}{}_{24}Bi^{3+}{}_2(O_{39}\square_1) - x(Bi_{24}Mn^{4+}{}_2O_{40})$ (line II) systems versus variable parameter of composition x. The error bars for x are standard deviations estimated in the structural refinement (Tables 3 and 4).

2 Crystals in the shape of a tetrahedron−cube combination were obtained from batches containing equimolar amounts of the $Na_2SiO_3 \cdot 9H_2O$ and $Mn(NO_3)_2 \cdot 6H_2O$ components. These crystals belong to space group $I23$ (Table 2). It is believed that the disorder in the crystal body is retained because faces of different simple forms are inequivalent in structure and, as a consequence, show different abilities for capturing of atoms in the course of crystal growth.[22]

It should be noted that mixed crystallographic positions populated by the cations that differ in crystal−chemical properties can serve as an indication that the phase is expected to undergo a kinetic phase transition accompanied by changes in the crystal symmetry and/or unit cell parameters. The ordering can result in a superstructure. In the compounds studied, dissymmetrization of the crystal structure due to the kinetic ordering does not change the structural type.

Conclusions

Deviations from the linear dependence of the unit cell parameters of the $Bi^{3+}{}_{24}M^{4+}{}_2O_{40}$ phases (M^{4+} = Si, Ge) on the radii of the atoms located at the tetrahedral position (M) provide support for the presence of vacancies (downward deviation) and Bi atoms (upward deviation) at this position in the $Bi_{24}(Si^{4+}{}_{1.48(4)}\square_{0.52})(O_{38.96(3)}\square_{1.04})$, $Bi_{24}(Mn^{4+}{}_{0.80(4)}\square_{1.20})$-$(O_{37.63(3)}\square_{2.37})$, and $Bi_{24}(Bi^{3+}{}_{0.94(4)}Mn^{4+}{}_{1.06})(O_{39.50}\square_{0.50})$ specimens.

Phases of the sillenite family containing Bi^{3+}, Si^{4+}, Mn^{4+}, and Mn^{5+} ions, and probably containing an admixture of Mn^{3+} ions, are synthesized in the $Bi_2O_3-SiO_2-MnO_2$ system and characterized by X-ray diffraction of single crystals and powders and IR spectroscopy. The presence of these ions is supported by deviation (or zero deviation) of the corresponding dots from the linear dependence of the unit cell parameters on the variable parameter of composition.

Dissymmetrization of the sillenite structure (lowering of the symmetry from $I23$ to $P23$ accompanied by a partial ordering of the phase) is found for the first time in the $Bi_{24}(Si^{4+}{}_{0.04(8)}$-$Bi^{3+}{}_{0.60}Mn^{4+}{}_{1.36})(O_{39.70}\square_{0.30})$, $Bi_{24}(Si^{4+}{}_{0.9(1)}Mn^{4+}{}_{1.1})O_{40}$, and $Bi_{24}(Si^{4+}{}_{0.17(1)}Bi^{3+}{}_{0.01}Mn^{4+}{}_{1.82})(O_{39.93(5)}\square_{0.07})$ phases in contrast to the $Bi_{24}(Si^{4+}{}_{1.48(4)}\square_{0.52})(O_{38.96(3)}\square_{1.04})$, $Bi_{24}(Si^{4+}{}_{1.1(1)}Bi^{3+}{}_{0.1}$-$Mn^{4+}{}_{0.8})(O_{39.95}\square_{0.05})$, and $Bi_{24}(Si^{4+}{}_{0.58(12)}Bi^{3+}{}_{0.02}Mn^{4+}{}_{1.40})$-$(O_{39.99}\square_{0.01})$ phases. This phenomenon is associated with the mixed structural positions shared by different atoms and conditions of crystal growth (crystallization under quasi-equilibrium hydrothermal conditions below 400 °C). The dependence of crystal morphology on the batch composition probably indicates that the batch composition affects the process of dissymmetrization.